EPJdirect (2003), to be processed by the editorial

EPJdirect
electronic only

The ALICE Dimuon Spectrometer

A. Morsch
on behalf of the ALICE Collaboration

CERN, 1211 Geneva 23, Switzerland
e-mail: andreas.morsch@cern.ch

Abstract. The ALICE forward muon spectrometer has been designed to measure the complete spectrum of heavy quark vector mesons via their muonic decays in pp, proton–nucleus (pA) and nucleus–nucleus (A–A) collisions. Here we present the main design criteria, an overview of the spectrometer and the status and plans of the project.

PACS: xxxx xxxx

1 Introduction

ALICE (A Large Ion Collider Experiment) is the detector dedicated to the study of nucleus–nucleus interactions at the LHC. It will investigate the physics of strongly interacting matter at extreme energy-densities [1]. In early 1995, the ALICE collaboration has launched a project to upgrade its central detector with a forward muon spectrometer to measure the complete spectrum of heavy-quark vector mesons (J/ψ, ψ', Υ, Υ', Υ'') via their muonic decay in pp, pA and heavy-ion collisions [2].

Heavy quarkonia states are hard, penetrating probes which provide an essential tool to study the earliest and hottest stages of heavy-ion collisions [3]. They can probe the strongly interacting matter created in these reactions on short distance scales and are expected to be sensitive to the nature of the medium, i.e. confined or de-confined [4], [5]. The suppression (dissociation) of the heavy-quark resonances is considered as one of the most important observables for the study of the QGP at the LHC (see Ref. [6] for a recent review).

In a de-confined medium, the quark–gluon plasma (QGP), quarkonium suppression is expected to occur due to the shielding of the binding potential by colour screening, leading to the break-up of the quarkonium states. The screening radius is inversely proportional to the energy-density. When it becomes smaller than the size of the resonance, the bound state cannot be formed anymore. Since the resonance size is inversely proportional to its binding energy excited states like ψ', Υ', and Υ'' are dissolved at lower energy-densities than their corresponding ground states J/ψ and Υ. More recent studies using lattice QCD show that the suppression of the less tightly bound states is not necessarily characteristic of the QGP but of the decrease of string tension as chiral symmetry restoration is approached [7] However, the most tightly bound state, Υ, will only be suppressed at energy densities reached at the LHC [8].

In addition to colour screening, quarkonia states will also be subject to nuclear absorption and possibly breakup by secondary hadrons. The relative size

of these effects have been extensively studied and debated at SPS energies. At the LHC energy it is expected that the J/ψ is formed far away from the nucleons thereby reducing the absorption effects. However, at this energy, other mechanisms than hard scattering like regeneration in the plasma or hadron phase could play a role in charmonium production and could even lead to a charmonium enhancement at the LHC.

From this sketch of quarkonium production and suppression at the LHC it is clear that a measurement of the complete spectrum of resonances, J/ψ, ψ', Υ, Υ' and Υ'' is essential. Moreover, the measurement has to be performed down to smallest transverse momenta to be sensitive to possible model dependent effects on the transverse momentum spectrum. The energy density dependence will be studied by varying the impact parameters and by studying in addition to the heaviest collision system (Pb–Pb) also intermediate mass and low mass A–A systems. To determine the primary production cross-section of the resonances and the amount of pre-resonance absorption, corresponding measurement have to be performed for pp and pA collisions.

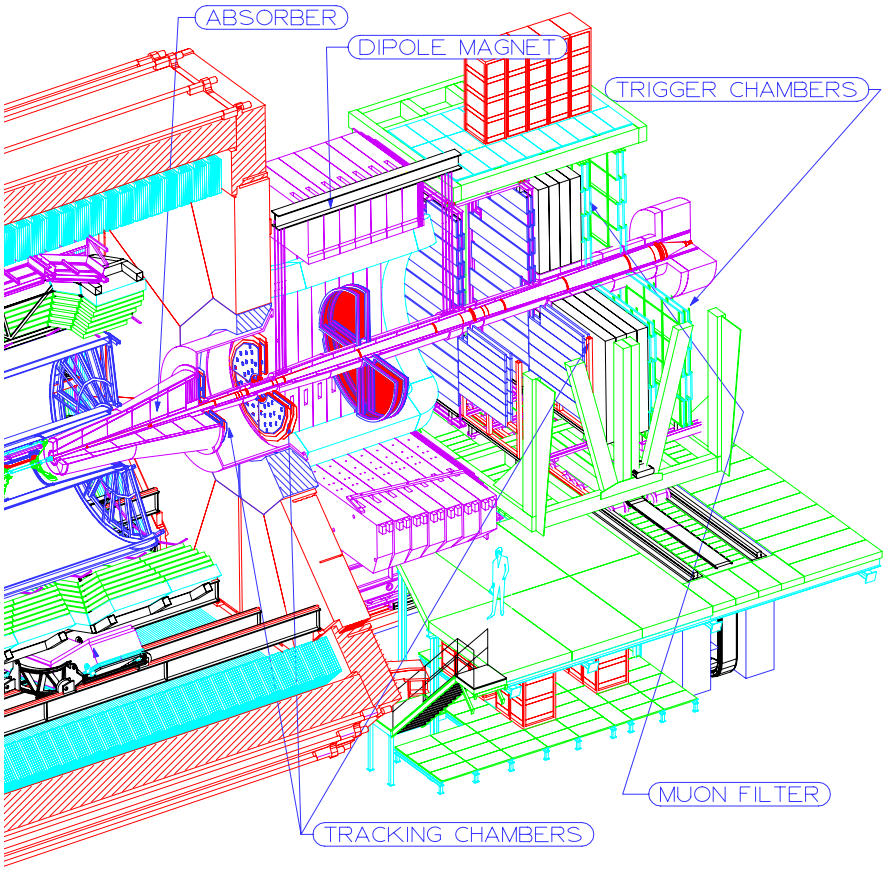

Fig. 1. Layout of ALICE with the forward muon spectrometer on the right side.

2 Design Criteria

The main design criteria of the dimuon spectrometer are driven by the following considerations:

- Low $p_{\rm t}$ acceptance for J/ψ production is essential since in this region direct production dominates. At high $p_{\rm t}$ a large fraction of J/ψs is produced via b-decays. Muon identification in the LHC environment is only feasible for muon momenta, p, above $3-4$ GeV/c because of the amount of material (absorber) required to reduce the flux of hadrons and muons from pion and kaon decays. Hence, measurement of low-$p_{\rm t}$ charmonia is possible only at small angles, θ, in the forward region, where the muons have sufficiently high momenta even at small $p_{\rm t}$. For the same reason, the life-time of pions and kaons is increased (Lorentz factor) so that they can be absorbed more efficiently before they decay into muons.
- As the accuracy of dimuon measurement with heavy nuclei will be statistics limited (at least for the Υ family), the spectrometer geometrical acceptance must be as large as possible.
- A resolution of 100 MeV/c^2 in the 10 GeV/c^2 invariant mass region is needed to resolve the Υ, Υ' and Υ''resonances. This requirement determines the bending strength of the spectrometer magnet as well as the space resolution and thickness of the muon tracking system.
- The spectrometer has to be equipped with a selective dimuon trigger system to match the maximum trigger rate of about 1 kHz handled by the DAQ maximising the number of high-$p_{\rm t}$ muons from rare processes that are written to tape.

3 Spectrometer Overview

The general layout of the Muon Spectrometer is shown in Fig.2. The angular acceptance of spectrometer covers the range $2^\circ - 9^\circ$ corresponding to a pseudo-rapidity range of $2.5 < \eta < 4.0$. Since it covers the forward direction, its design is similar to solutions used in fixed target experiments. The important difference is that the forward particle flow from the primary interaction, that carries the largest fraction of the collision energy, cannot be absorbed in a beam plug because the beam pipe passes through the spectrometer. Instead, the particles have to be absorbed in a dense shield (Pb, W) which surrounds the beam pipe decreasing the hit rate from secondary interactions to an acceptable level. The amount of shield needed in the radial direction to sufficiently suppress lateral punch-through determines the minimum angle at which muons can be measured. The upper bound is a compromise between acceptance and detector costs scaling with size.

The front absorber has a total of 11 $\lambda_{\rm I}$ and consists of layers of carbon, concrete and steel. The outer surface of the absorber is covered by heavy materials

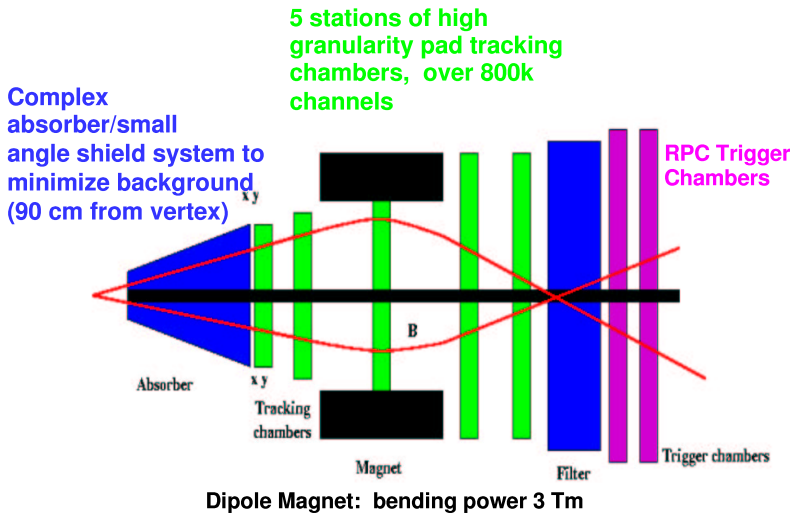

Fig. 2. Layout of the muon spectrometer.

(Pb and W) in order to shield the central detectors against background particles from secondary interactions. At small angles it is followed by a beam shield (small angle absorber).

The tracking system consists of 10 planes of thin high-granularity tracking chambers arranged in 5 stations of two planes each. A resolution of $< 100\,\mu$m is required in the bending plane of the dipole magnet (about 2 mm in the non-bending plane) to achieve the required mass resolution of 100 MeV at the Υ mass. For the same reason the average thickness of the chambers should not exceed 3% of X_0. The granularity has to be chosen to cope with hit densities up to $0.1\,\mathrm{cm}^{-2}$. Cathode pad and strip chambers with segmentation of both cathode planes are used.

One tracking station is placed inside a large dipole magnet with a field integral of $B.l = 3\,\mathrm{Tm}$ and a maximum field strength of 0.7 T. Two stations are placed before and two behind the magnet. Momentum measurement is performed using a combined angle–angle and sagitta measurement.

The trigger system consists of a passive muon filter ($11\,\lambda_\mathrm{I}$ of Fe) followed by four planes of trigger chambers, Resistive Plate Chambers (RPCs).

In the following sections the technology choice for the various spectrometer components is described in some more details.

4 Technology choices, status and plans

4.1 Tracking chambers

The design of the tracking system is driven by three main requirements:

- The space resolution of about 100 μm in the bending plane (about 2 mm in the non-bending plane), which is needed to achieve the desired invariant mass resolution of 100 MeV/c^2 in the Υ mass region.
- For the same reason the chambers have to be thin in order to keep the multiple scattering in the chambers at a minimum.
- The chambers must have the capability to operate in presence of a high particle multiplicity. For central Pb–Pb collisions, a few hundred particles are expected to hit each muon chamber. A maximum hit density of about 5×10^{-2}cm^{-2} is reached at low radii, i.e. close to the beam shield.

Moreover, the tracking system has to cover a total surface of almost 100 m^2. All these requirements can be fulfilled using cathode pad chambers. These are arranged in five stations: two are placed before, one inside and two after the dipole magnet. Each station is made of two chamber planes. Each chamber has two cathode planes, which are both segmented and read out to provide two-dimensional hit information. The number and position of the stations have been optimized for mass resolution and allow for angle and sagitta measurement of the momentum.

To keep the occupancy at the 5% level, a large segmentation, i.e. small size of the readout pads and strips, is needed. For instance, pads as small as 4.2×6 mm^2 are required for the first chamber in the region close to the beam pipe, where the highest multiplicity is expected. Since the hit density decreases with the distance from the beam, larger pads are used at larger radii. This allows to restrict the total number of channels to about one million. To reduce the multiple scattering of the muons in the chamber material, special care was taken in their design based on the choice of composite materials (e.g. carbon fiber) and foams to guarantee their rigidity [9]. This allows to limit the chamber thickness to about $0.03X_0$ (Fig. 3).

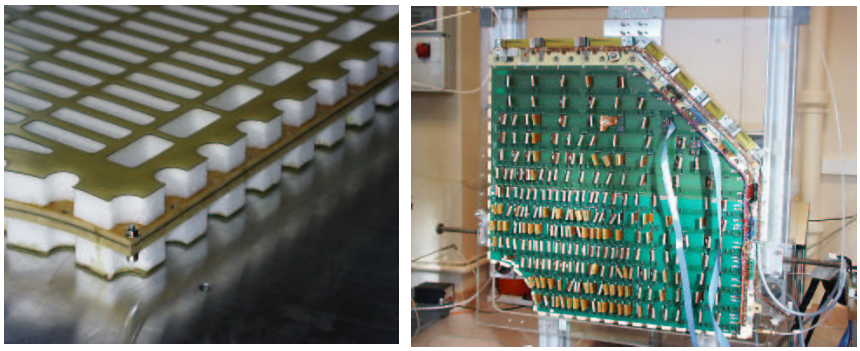

Fig. 3. Mechanical structure of Station 1 and 2 (left) and full quadrant of Station 1 (right).

Due to the different size of the stations, ranging from few square meters for station 1 to more than 30 m^2 for station 5, two different designs have been

adopted. The first two stations are based on a quadrant structure, with the readout electronics spread out on their surface. For the remaining stations a slat architecture has been chosen. The maximum size of the slat is 40×280 cm^2 and the electronics sit on the side of the slats [10]. All slats overlap to avoid dead zones on the detector.

Extensive tests on small size and full size prototypes, both for the quadrant and the slat architecture, have shown that these detectors achieve the required performances. In particular, space resolutions of better than 70μm have been measured.

For all tracking stations, the front-end electronics board (MANU) comprises the following modules and functionalities: the analog part (MANAS) provides charge amplification, filtering, shaping, track & hold and a 16–1 analog multiplexer, 12-bit ADCs (AD7476) convert the analog signals into digital ones and the readout chip (MARC) provides zero-suppression and the interface to the data acquisition.

The first full quadrant of the Station 1 has been tested at the CERN PS in July 2002. It consists of a 0.7 m^2 frame-less structures, 14 000 electronics channels per cathode and uses a gas mixture of 80% Ar+20% CO_2. It has three segmentation zones with different pad sizes. The data have shown gain variation across the detector of up to a factor of three. Further investigations in the laboratory using source tests and mechanical survey have lead to the conclusion that the chamber does not possess sufficient mechanical stability. It turns out that the problem can be solved by improving the closing procedure during assembly and by increasing the stiffness using a central spacer. A new full quadrant of the station 1 should be ready by November 2003.

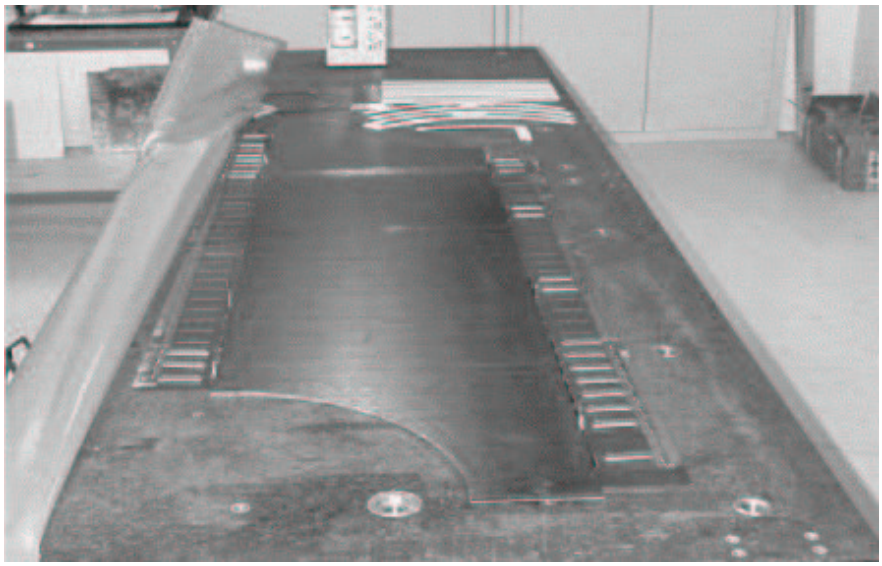

Fig. 4. Rounded slat.

For the stations 3, 4 and 5, the PCBs of the standard slats have been validated and all the components, carbon sandwiches, spacers, PCBs, and bus-bars, are being fabricated. The production will start at the beginning of September 2003 with the fabrication of one qualification slat at each of the four production sites. A rounded slat (Fig. 4) which is located around the beam shield will be tested in beam in July 2003. Start of slat mass production is foreseen before end of 2003.

A first batch of 2000 preamplifiers (MANAS) has been delivered and 250 chips have been mounted on MANU boards which are currently under tests. A last iteration of the MARC chip was launched in May 2003 and a first batch should be available by October.

4.2 Trigger

In central Pb–Pb collisions, about eight low-p_{t} muons emitted predominantly in pion and kaon decays are expected to be detected in the spectrometer. In order to reduce the trigger rate to an acceptable level a p_{t}-cut is applied at the trigger level.

A dimuon trigger signal is issued when at least two tracks above a pre-defined p_{t} threshold are detected in an event. This is achieved by correlating the position and angle of tracks recorded by the trigger planes. Together with the vertex constraint this procedure yields the deflection in the dipole and hence a momentum measurement. According to simulation results, a "low" p_{t} cut (1 GeV/c) can be used for J/ψ and a "high" p_{t} cut (2 GeV/c) for Υ selection.

To perform the p_{t} cut, a position-sensitive trigger detector with space resolution not worse than 1 cm is needed. This resolution is achieved by single gap Resistive Plate Chambers (RPCs) operated in streamer mode[12]. The trigger system consists of four RPCs planes arranged in two stations separated by 1 m and placed behind the muon filter (1.2 m of iron). The total active surface is about 150 m^2. The $x-y$ coordinates of the RPC hits are readout by segmented strips. Pitch and length of the strips increase with their distance from the beam axis approximately in the same proportion as the background hit rate decreases. The RPCs are equipped with dual-threshold front-end discriminators (ADULT), designed to improve the timing properties of the detector and match the time resolution (1–2 ns) needed for the identification of the bunch crossing. From the discriminators, the signals are sent to the trigger electronic (local trigger cards, based on programmable circuits working in pipeline mode) where the coordinate measured in the first and second stations are compared to determine the muon p_{t}. Owing to the short decision time (600 – 700 ns) of the electronics, the dimuon trigger participates to the ALICE Level 0 trigger.

The maximum expected hit rate is 40 Hz/cm^2 for Ar–Ar high luminosity runs. In pp runs, where an important contribution comes from beam–gas interactions a hit rate of 10 Hz/cm^2 is expected. To achieve the required rate capability, RPC electrodes are made of low-resistivity BAKELITE ($\rho \sim 3\times10^9$ Ωcm).

Long-term irradiation of small and full scale prototypes have been performed at the GIF (Gamma Irradiation Facility) since 2001 [13]. Some prototypes have a thin double-layer of linseed oil which reduces aging and were operated with and without adding a small amount of humidity to the gas. Several detectors

tested in these conditions proved to be still efficient after having integrated a charge equivalent to a few ALICE-years of data taking. Preliminary results show that the best chambers are those with a double layer of line-seed oil and dry gas with a 1% SF_6 contents. However, the operation of the detector strongly depends upon the background from beam–gas interactions in pp collisions, where ALICE operates at low luminosity but full beam intensity.

The final front-end chips, which have been specially designed for the streamer mode, and front-end boards have been successfully operated in various test beams since 2001. The test bench for their mass production is ready. A reduced size prototype of the muon trigger setup, including detector, front-end and trigger electronics, has been operated at the GIF in June 2002 and has shown an excellent detection efficiency and background rejection capability. In the near future, a full scale RPC, fully equipped, will be tested at GIF.

The hardware level 0 trigger is followed by the high-level trigger system (HLT) [11]. In the simplest case a trigger issued by the trigger chambers is associated with regions of interest (RoI) on the two tracking chambers in front of the trigger wall. Clusters found in the RoIs are matched to the trigger hits and interpolated to the interaction point to yield an improved transverse-momentum measurement. In this way 80% of false triggers at low-p_t can be rejected largely improving the low-p_t physics capabilities.

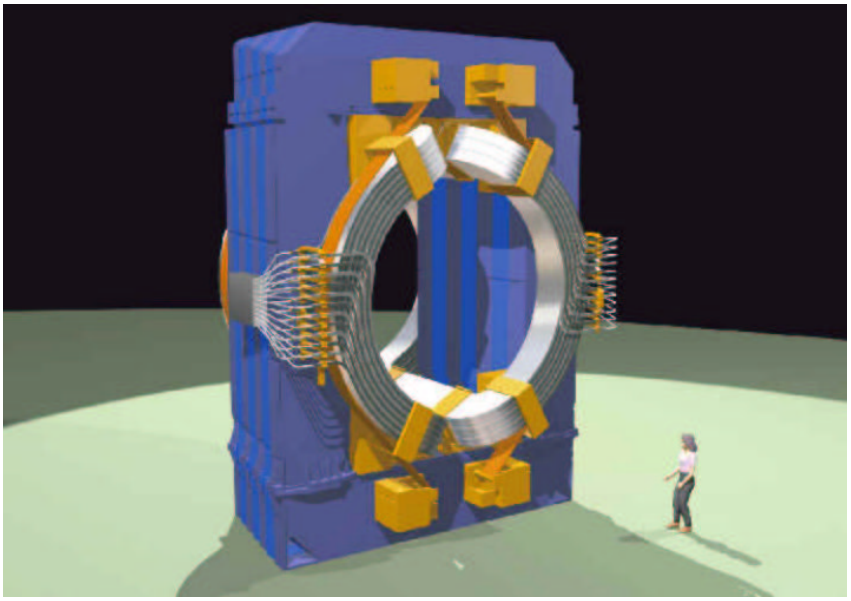

Fig. 5. Dipole magnet.

4.3 Dipole Magnet

The dipole magnet [14] with resistive coils is placed at about 7 m from the interaction vertex, just outside the L3 magnet. Its size (free gap between poles ∼3.5 m, height of the yoke ∼9 m, total weight about 850 t) is defined by the requirements on the angular acceptance of the spectrometer. Its magnetic strength ($B_{\rm nom}$= 0.7 T, 3 Tm field integral between the interaction point and the muon filter) is defined by the requirements on the mass resolution.

The horizontal factory assembly of the yoke has been finished in December 2002. The inspection and survey gave globally satisfactory results [15] and yoke components are now being prepared for shipping to CERN. A dummy coil pancake has been successfully produced in October 2002. All coil manufacturing tooling has been produced and tested and coil production has started in January 2003. The manufacturing contracts for the coil supports have been attributed and its delivery is scheduled for July 2003. A temporary foundation has been installed at the pre-assembly site for the magnet.

The transport of the yoke components to CERN shall take place in June 2003. The pre-assembly in the UX25 cavern will be terminated after delivery of the coils at the end of August 2003. Pre-commissioning work including power tests and magnetic-field checks are planned from October until end 2003.

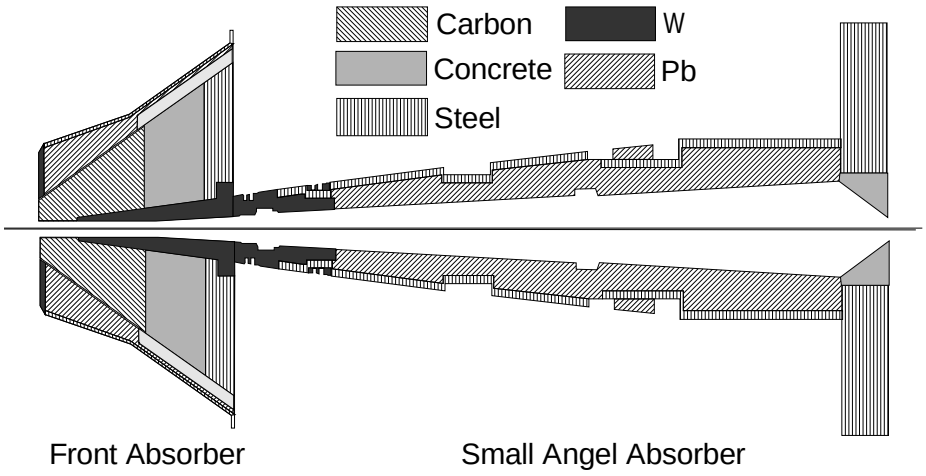

Fig. 6. Layout of the front and small-angle absorbers.

4.4 Absorber System

The purpose of the front absorber is to suppress as much as possible the number of muons from pion and kaon decays which represent an important physics background and at the same time to reduce the hit rate on the tracking chambers due to punch-through. A compromise between absorption capability and multiple scattering of the muons which limits the angular resolution is found

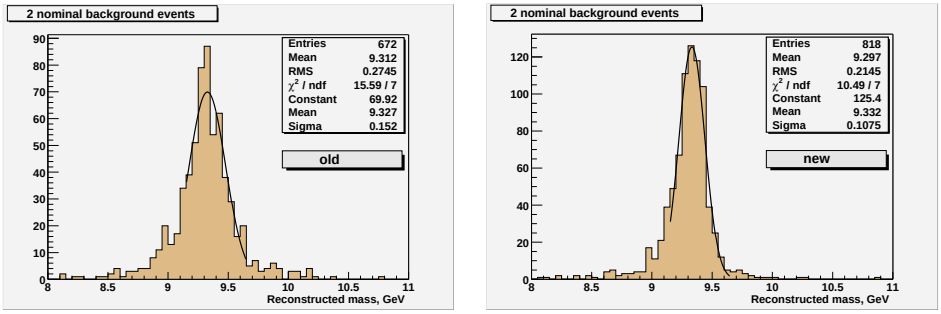

Fig. 7. Reconstructed dimuon mass spectrum from Υ decays. The hits resulting from muons have been merged with the background from two central HIJING events. Whereas with the old cluster finder the mass resolution degrades (left spectrum) with the MLEM algorithm it stays close to the nominal value (right spectrum).

by placing low-Z materials close to the interaction point and high-Z materials close to the first chambers. In case of ALICE, the absorber consists of a sequence of carbon, concrete and steel. The outer surface of the absorber is made out of dense material in order to shield other detectors from background particles.

The inner part of the front absorber, outside of the spectrometer acceptance is made out of dense material (W) in order to absorb particles from interactions in the beam pipe. This beam shield is continued outside the front absorber where its inner surface follows an opening cone until the end of the spectrometer where the cone closes back to the radius of the beam pipe. This open geometry has been found to be the optimal solution for such an absorber system.

Recently the absorber system has been complemented by an Al-disk, 20 cm thick, covering the free region between the outer radius of the front absorber and the inner radius of the L3 door. The purpose of this disk is to absorber particles produced in the central part of ALICE curling due to the magnetic field into the spectrometer acceptance.

The mechanical design of the front absorber has been completed. Only some stability issues in case of earthquake for its support structure (FASS) have to be solved. Also the design of the beam shield (Small-Angle Absorber, SAA) has been almost completed after many iterations. The design of the SAA represents a complex integration task since its inner surface interfaces with the vacuum system (pipe, bake-out jacket, bellows and flanges) and its outer surface with the tracking chambers. Most importantly the integration had to be performed respecting the requirement of keeping the background rate at an acceptable level [16].

In October 2003 the heavy parts made out of tungsten, lead and iron will be delivered. The installation of the front absorber support structure will start in January 2004. The front absorber and small-angle absorber will be assembled from May to September 2004 and installed from October to November of the same year.

5 Physics Performance

The basic physics performance of the dimuon spectrometer has been documented in the Technical Proposal and Technical Design reports [2]. It has been demonstrated that the required mass resolutions can be achieved and that acceptances as well as reconstruction and trigger efficiencies are high enough to detect all resonances with sufficient significances [17]. Detailed studies for the ALICE Physics Performance Report to be published in 2003/2004 are ongoing. An important open question was the dependence of the mass resolution and the reconstruction efficiency on the background hit rate. Earlier studies have shown that efficiency and mass resolution decrease significantly with the chamber occupancy when the number of overlapping clusters increases. This was due to imperfections of the cluster deconvolution algorithm. Recently a new cluster finder algorithm based in maximum likelihood expectation maximization (MLEM) [18] has been implemented and gives very satisfying results [19].

Fig. 7 shows the reconstructed dimuon mass spectrum from Υ decays. The hits resulting from muons have been merged with the background from two central HIJING events. Whereas with the old cluster finder the mass resolution degrades (left spectrum) with the MLEM algorithm it stays close to the nominal value (right spectrum).

6 Conclusions

ALICE is building a forward muon spectrometer which will measure the complete spectrum of heavy quark vector mesons via their muonic decays in pp, proton-nucleus (pA) and nucleus-nucleus (AA) collisions. The dimuon spectrometer project is overall in a good shape. Some production has already started and the remaining should begin in 2003.

References

1. Y. Schutz: proceedings of this conference;
   C. Blume: proceedings of this conference.
2. ALICE Collaboration, Addendum to the Letter of Intent, CERN/LHCC 95-24;
   ALICE Collaboration, Addendum to the Technical Proposal, CERN/LHCC 96-32;
   ALICE Collaboration, Technical Design Report of the Dimuon Forward Spectrometer , CERN/LHCC 99-22;
   ALICE Collaboration, Addendum to the Technical Design Report of the Dimuon Forward Spectrometer ,CERN/LHCC 2000-046.
3. H. Satz: Proc. Quark Matter 95, Nucl. Phys. **A590** (1995) 63c.
4. T. Matsui and H. Satz: Phys. Lett. **B178** (1986) 416.
5. D. Kharzeev and H. Satz, Phys. Lett. **B334** (1994) 155.
6. B. Alessandro et al.: ALICE Internal Note, 2002-025 (2002) 34-36.
7. S. Digal, P. Petreczky and H. Satz: Phys. Rev. **D64** (2001) 094015;
   S. Digal, P. Petreczky and H. Satz: Phys. Lett. **B514** (2001) 57.
8. J.F. Gunion and R. Vogt: Nucl. Phys. **B492** (1997) 301.
9. P.Battacharya et al.: Internal Note ALICE-INT-2003-003.

10. H. Borel et al.: Internal Note ALICE-INT-2002-023;
C. Cicalo et al.: Internal Note ALICE-INT-2002-17.
11. F. Manso. Internal Note ALICE-INT-2003-04.
12. R. Arnaldi et al: Nucl. Instr. and Meth. **A490** (2002) 51 and ref. therein.
13. A. Ferretti et al.: Proceedings of the VI Workshop on Resistive Plate Chambers and Related Detectors, Coimbra, Nov. 26-27 2001, to be published on Nucl. Instr. and Meth. A.
14. D. Swoboda: ALICE Muon Arm Dipole Magnet Conceptual Design Report, Internal Note ALICE-INT-1998-10-13.
15. S. Evrard and D. Swoboda: Internal Note ALICE-INT-2003-005.
16. J.P.Cussonneau et al.: Internal Note ALICE-INT-98-27;
V.F.Basmanov et al.: Internal Note ALICE-INT-1999-38;
A. Morsch: Internal Note ALICE-INT-2002-18.
17. P. Crochet: EPJdirect C, 4(S1) (2002) 22.
18. L.A. Shepp and Y. Vardi: IEEE Trans. Med. Im., v.1 (1982) 113.
19. A. Zintchenko et al.: Internal Note ALICE-INT 2003-02-19.